TITLE

Morphology of subcortical brain nuclei is associated with autonomic function in healthy humans

SHORT TITLE/RUNNING HEAD

Subcortical morphology & autonomic function

AUTHORS & AFFILIATIONS

James K. Ruffle (1,2), Steven J. Coen (3), Vincent Giampietro (4), Steven C.R. Williams (4), A. Vania Apkarian (5), Adam D. Farmer (1,6)* & Qasim Aziz (1)*

1. Centre for Neuroscience and Trauma, Blizard Institute, Wingate Institute of Neurogastroenterology, Barts and the London School of Medicine & Dentistry, Queen Mary University of London, 26 Ashfield Street, London, E1 2AJ, UK

2. Medical Acute Assessment Unit, Royal London Hospital, Barts Health NHS Trust, Whitechapel Road, Whitechapel, London, E1 1BB, UK.

3. Research Department of Clinical, Educational and Health Psychology, University College London, Gower Street, London, WC1E 6BT, UK

4. King's College London, Institute of Psychiatry, Psychology & Neuroscience, Department of Neuroimaging, London, SE5 8AF, UK

5. Department of Physiology, Northwestern University, Feinberg School of Medicine, Chicago, Illinois, 60611, USA

6. Department of Gastroenterology, University Hospitals Midlands NHS Trust, Stoke on Trent, Staffordshire, ST4 6QG, UK

Corresponding Author: Professor Qasim Aziz

ARTICLE TYPE

Original article

WORD COUNT

Abstract 249;

Main document: Introduction 566; Methods 1424; Results 378; Discussion 1687; References: 1913

PAGE COUNT

32

FIGURE / TABLE / MULTIMEDIA COUNT

Figures 6; Tables 1; Multimedia Videos 2

ADDRESS FOR CORRESPONDENCE

Professor Qasim Aziz, PhD FRCP

Wingate Institute of Neurogastroenterology, 26 Ashfield Street, London, E1 2AJ, UK

Tel: - +44 (0) 2078822644, Email: - q.aziz@qmul.ac.uk

KEY WORDS

Cardiac vagal tone, cardiac sympathetic index, sympathetic nervous system, parasympathetic nervous system, autonomic nervous system, brain structure, vertex analysis, structural morphometry

CONFLICT OF INTERESTS

The authors have no conflicts of interest to declare.

*Adam D Farmer & Qasim Aziz are joint senior co-authors.

ABSTRACT

The autonomic nervous system (ANS) is a brain body interface which serves to maintain homeostasis by influencing a plethora of physiological processes, including metabolism, cardiorespiratory regulation and nociception. Accumulating evidence suggests that ANS function is disturbed in numerous prevalent clinical disorders, including irritable bowel syndrome and fibromyalgia. Whilst the brain is a central hub for regulating autonomic function, the association between resting autonomic activity and subcortical morphology has not been comprehensively studied and thus was our aim. In 27 healthy subjects (14 male and 13 female; mean age 30 years (range 22 – 53 years)), we quantified resting ANS function using validated indices of cardiac sympathetic index (CSI) and parasympathetic cardiac vagal tone (CVT). High resolution structural magnetic resonance imaging scans were acquired, and differences in subcortical nuclei shape, i.e. "deformation", contingent on resting ANS activity were investigated. CSI positively correlated with outward deformation of the brainstem, right nucleus accumbens, right amygdala and bilateral pallidum (all thresholded to corrected $p<0.05$). In contrast, parasympathetic CVT negatively correlated with inward deformation of the right amygdala and pallidum (all thresholded to corrected $p<0.05$). Left and right putamen volume positively correlated with CVT *(*$r=0.62$, $p=0.0047$ and $r=0.59$, $p=0.008$, respectively), as did the brainstem ($r=0.46$, $p=0.049$). These data provide novel evidence that resting autonomic state is associated with differences in the shape and volume of subcortical nuclei. Thus, subcortical morphological brain differences in various disorders may partly be attributable to perturbation in autonomic function. Further work is warranted to investigate these findings in clinical populations.

Corresponding Author: Professor Qasim Aziz

INTRODUCTION

The autonomic nervous system (ANS) is a bidirectional brain-body interface that serves to integrate changes in the external environment with the internal milieu and maintain homeostasis. Comprising of two broadly opposing arms, the sympathetic (SNS) and parasympathetic nervous systems (PNS), the functions of the ANS are considerable, spanning from metabolic control to cardiorespiratory regulation and pain processing (Farmer, et al., 2014b). Whilst it is well documented that the brain is the central hub for the regulation of autonomic function, the use of neuroimaging to investigate the association between brain morphology and autonomic function, not least with advanced neuro-analytical techniques, is far from comprehensive.

The main branch of the PNS is the vagus nerve. Although the vagus is predominantly composed of afferent nerves, the efferent arm is postulated to play a pivotal role in modulating visceral nociception (Botha, et al., 2015), gastrointestinal motility (Frokjaer, et al., 2016) cardioregulation (Bonaz, et al., 2013), and inflammation (Bonaz, et al., 2016; Matteoli, et al., 2014). Similarly, the SNS, due to its multiple interactions with the peripheral and central nervous system, may also influence peripheral inflammation and nociception (Schlereth and Birklein, 2008).

Advances within autonomic neuroscience have facilitated the development of many techniques to quantitatively assess autonomic function, such as the evaluation of heart rate variability (HRV). Amongst such measurements to objectively quantify SNS and PNS activity are the cardiometrically derived parameters, referred to as cardiac sympathetic index (CSI) and cardiac vagal tone (CVT) respectively. In contrast to the traditional derivation of

autonomic activity, such as by HRV, both CSI and CVT yield superior temporal resolutions and have been associated with multiple neurophysiological functions, including pain processing and the neuro-endocrine-immune axis (Denver, et al., 2007; Farmer, et al., 2014b; Ruffle, et al., 2017). Moreover, abnormal resting SNS and PNS activity has been reported in a number of clinical disorders such as functional chest pain (Hoff, et al., 2016), irritable bowel syndrome (IBS) (Spaziani, et al., 2008), inflammatory bowel disease (Bonaz, et al., 2013), fibromyalgia (Martinez-Martinez, et al., 2014), Ehlers-Danlos syndrome (De Wandele, et al., 2014) and diabetes mellitus (Vinik, et al., 2003).

Similarly, developments in neuroimaging analytical methods, using Bayesian vertex analysis, have facilitated the investigation of shape differences across subcortical nuclei depending on a given variable (referred to as "deformation"), which do not purely encompass volumetric delineation (Patenaude, et al., 2011). For example, this novel technique has provided insights into the effect of diabetes mellitus and psychosis on the shape of subcortical structures (Dean, et al., 2016; Zhang, et al., 2016). This is in contrast to the reductionist approach offered by more basic morphological analyses which reduces a complex brain region to a mere volume. Furthermore, Patenaude *et al.* suggest that this Bayesian shape analysis modality avoids many limitations of pre-existing structural neuroimaging preprocessing, including the lack of dependency on tissue classification methods and smoothing processes (Patenaude, et al., 2011).

To date, no studies have investigated the link between resting autonomic indices and subcortical nuclei shape, despite evidence that subcortical regions influence autonomic control (Bonaz, et al., 2016; Farmer, et al., 2013a; Park and Thayer, 2014). As no studies have

directly investigated how resting CSI and CVT relate to subcortical brain volume or shape, we thus aimed to address this knowledge gap. We hypothesized that subcortical nuclei would significantly differ in shape based upon resting CSI and CVT, whilst they may not differ in terms of total regional volume.

MATERIALS & METHODS

SUBJECTS

Twenty-seven subjects (14 male and 13 female; mean age 30 years (range 22 – 53); all right handed) were recruited by local advertisement. Subjects were asked to refrain from alcohol and caffeine consumption in the preceding 24 hours before the study to limit exogenous confounders of resting autonomic indices (Hibino, et al., 1997; Volkman, et al., 2015). All subjects were screened for subclinical anxiety and depression by means of the Hospital Anxiety and Depression Scale (Zigmond and Snaith, 1983), and were excluded if a score of ≥ 8 was recorded to prevent an anxiety-related confound on vagal tone (Chen, et al., 2012; Kollai and Kollai, 1992). The study was approved by the Queen Mary, University of London ethics committee (ref CREC/07/08-7) and all subjects were modestly remunerated and provided written consent prior to taking part in the study. This study utilized data that were previously acquired by our group (Farmer, et al., 2013a; Ruffle, et al., 2015b).

AUTONOMIC MEAURES

Electrocardiogram (ECG) electrodes (Ambu Blue Sensor P, Denmark) were placed at the cardiac apex, left and right sub-clavicular areas of each subject for electrical signal acquisition. Subsequently, ECG readings were digitally recorded using a biosignals acquisition system

(Neuroscope, Medifit Instruments, Enfield, Essex, UK) at 5 kHz. Autonomic parameters were recorded as per international recommendations (European, et al., 1996). For each subject, mean digital arterial blood pressure (MBP) was measured non-invasively using a validated photoplethysmographic technique (Portapres, Amsterdam, Netherlands) (Benarroch, et al., 1991; Eckert and Horstkotte, 2002).

SYMPATHETIC NERVOUS SYSTEM: CARDIAC SYMPATHETIC INDEX

Resting SNS activity was quantified by means of CSI (Farmer, et al., 2013b). To undertake this, firstly R-R interval data was extracted from ECG recordings and were hand edited to remove any missed, or extra beats, as per accepted recommendations as these can otherwise result in large artefacts (European, et al., 1996). Subsequently, R-R data was transferred to the Cardiac Metric Program (CMet, University of Arizona, Arizona, USA), which calculates the validated Toichi's cardiac sympathetic index (Toichi, et al., 1997). CSI is a numerical ratio of R-R intervals and thus has no units.

PARASYMPATHETIC NERVOUS SYSTEM: CARDIAC VAGAL TONE

Resting efferent PNS activity was determined by CVT, and is described in detail elsewhere (Farmer, et al., 2014b). In brief, to quantify resting vagal tone in each subject, the incoming QRS complex is compared to a unique template, generated from the initial ECG acquisition stages of the individual. If the QRS complexes are sufficiently comparable, voltage gated oscillators within the Neuroscope generate a 1 mV pulse, which feeds to a two-limb circuit, consisting of a high-pass and low-pass limb. The high-pass limb precisely follows the incoming QRS signal, whilst the low-pass limb produces a damped rendition (Little, et al., 1999). Therefore, the lesser the delta change of an incoming signal, that is to say the lower the HRV,

the closer the low-pass limb will mimic that to the high-pass, resulting in a lower value. In contrast, the greater the HRV the more the low-pass limb will deviate from its high-pass counterpart, resulting in a higher value. This phenomenon is referred to as 'phase shift demodulation', and is uniquely based upon non-invasive measures of PNS tone. CVT is measured on a linear vagal scale (LVS), where a value of 0 is derived from fully atropinized healthy human volunteers (Julu, 1992; Julu and Hondo, 1992). CVT has been demonstrated to closely correlate (r>0.75, p<0.0001) with more traditional measures of HRV, including those derived from frequency domain analysis (Brock, et al., 2017).

All subjects were studied in the afternoon (between 14:00-16:00) in a temperature controlled (20-22°C), constantly lit, quiet laboratory. Female participants were only studied during the follicular phase of their menstrual cycle, so as to limit for menstrual period and hormonal confounds previously documented in studies of resting autonomic activity (Brar, et al., 2015). Subjects were reclined at 45° on a bed. After attachment of all autonomic recording apparatus, a 20-minute period ensued whereby each subject was told to 'rest' during which baseline CSI and CVT were derived. Previous studies have shown baseline autonomic function, including CVT, to be highly reproducible over time (Kano, et al., 2014), and thus mean CSI and CVT values were derived from this resting period and their relationship to structural brain scans were explored.

STRUCTURAL MRI DATA ACQUISITION

Magnetic resonance imaging (MRI) data were acquired using a General Electric SIGNA HDx 3.0 Tesla scanner, fitted with an 8-channel, phased-array receive-only head coil, located at the Centre for Neuroimaging Sciences, Institute of Psychiatry, Psychology & Neuroscience,

King's College London. Head movement was minimised by application of foam padding within the head coil. High resolution T1-weighted 3D FSPGR structural scans were acquired in sagittal orientation using the following parameters: repetition time (TR) 7.02 ms; echo time (TE) 2.82 ms, inversion time (TI) 450 ms; slice thickness 1.1 mm; field of view 280 mm; flip angle 20°; spatial positions 196; image matrix 256 x 256 x 196 voxels; in plane voxel dimensions 1.1 x 1.1 x 1.1 mm.

STRUCTURAL MRI PRE-PROCESSING

MRI pre-processing was undertaken using the FMRIB Software Library (FSL) analysis package (version 5.09, http://fsl.fmrib.ox.ac.uk/fsl) (Smith, et al., 2004). Raw structural MRI images were first carefully manually reviewed, to check for signal and image artefact that may otherwise confound findings. Following this, vertex (shape) and volumetric analyses were performed using FSL-FIRST 5.0, a Bayesian modelling analytical toolkit developed for segmentation, shape and volumetric analysis of subcortical brain regions (see (Patenaude, et al., 2011)) (Figure 1) (Movie 1) (also see http://fsl.fmrib.ox.ac.uk/fsl/fslwiki/FIRST/UserGuide). Firstly, the software package utilises the FSL brain extraction tool (BET), which removes outlying skull and cerebrospinal fluid (CSF) that may otherwise confound image data. Following this, FSL-FIRST permits the segmentation of each subject's structural scan into 15 subcortical structures, comprising the bilateral nucleus accumbens, amygdala, caudate, hippocampus, pallidum, putamen and thalamus, along with the brainstem in its entirety. Segmented structures were registered to the Montreal Neurological Institute (MNI) 152 1mm template for high resolution analysis with control for total brain volume. All segmentations were manually reviewed for error prior to analytical use. The segmented brainstem data of one subject was rejected on the grounds of

segmentation error. Each resultant subcortical nuclei file was concatenated to a single 4D structural file (1 volume per subject) to permit statistical analysis. In addition to vertex-wise analysis, subcortical volume analysis was conducted by extracting subcortical volumes using FSL-STATS. This resulted in a volumetric count, in mm^3, for each of the 15 subcortical regions for all subjects.

[INSERT FIGURE 1 HERE]

[INSERT MOVIE 1 HERE FOR ONLINE VERSION]

DATA ANALYSIS

STATISTICAL ANALYSIS OF STRUCTURAL MRI DATA

Linear contrast analyses were performed using the FSL-RANDOMISE statistical software, a permutation inference method that is currently described as the optimum statistical analysis method for vertex-wise analysis of structural data (Winkler, et al., 2014). Using a general linear model (GLM) we investigated potential linear correlations between pre-processed FSL-FIRST subcortical vertex data and both resting CVT and CSI at the individual level (both positive and negative association). Both age and gender were added as demeaned covariates to limit confounds on both nuclei structural morphology, as well as total brain volume and the remaining resting autonomic index not investigated for the particular GLM (i.e. when investigating for CVT-associated structural changes, CSI was added as a covariate and *vice versa*) (Farmer, et al., 2014b; Mumford, et al., 2015). The total number of permutations was automatically calculated by the FSL-RANDOMISE software, and was deemed to be 5040, with family-wise error (FWE) correction methods additionally employed as per the FSL-FIRST user guidelines (see http://fsl.fmrib.ox.ac.uk/fsl/fslwiki/FIRST/UserGuide). Two-dimensional

threshold free cluster enhancement (TFCE) correction was also used, as per guidelines. This method produces a vertex map for each subcortical region of *t* statistics at the voxel level which can then be thresholded to a given value of alpha. A statistical threshold of $p < 0.05$ was applied for the criterion of statistical significance, and only TFCE corrected results are reported herein.

STATISTICAL ANALYSIS OF DEMOGRAPHIC & AUTONOMIC DATA

Data distribution of CVT and CSI were analyzed using the D'Agostino-Pearson omnibus K2 normality test and visual inspection of histograms (D'Agostino and Stephens, 1986). Dependent on this outcome, data are presented either as mean ± standard deviation (SD) for parametric data, or median with interquartile range (IQR) for non-normally distributed data. Correlational analyses were performed using Pearson or Spearman's coefficient as appropriate. All tests were two-tailed, with $p < 0.05$ adopted as the criterion for statistical significance. Statistical analyses were performed using MATLAB (version 2016a, uk.mathworks.com) and GraphPad Prism (version 6.00, GraphPad Software, La Jolla California, USA, www.graphpad.com).

RESULTS

DEMOGRAPHIC & AUTONOMIC DATA

The mean age of the cohort was 30 years (range 22-53), and consisted of 14 male and 13 female subjects (Table 1). Mean ± standard deviation resting heart rate was 68 ± 10.65 beats per minute. Mean resting systolic blood pressure was 139 ± 34.70 mmHg, whilst mean diastolic blood pressure was 66 ± 15.66 mmHg, likely attributable to experimentally-induced anxiety. Mean resting CVT was 9.13 ± 4.70 (Figure 2a), whilst mean resting CSI was 2.26 ± 0.76

(Figure 2b). Resting CVT was significantly negatively correlated with resting HR (r = -0.63, p=0.0004). There was no significant association between demographical data, including age or gender, and autonomic parameters including HR, CVT or CSI (Figure 2, Table 1).

[INSERT FIGURE 2 HERE]

[INSERT TABLE 1 HERE]

SUBCORTICAL SHAPE ANALYSIS

SYMPATHETHIC: CARDIAC SYMPATHETIC INDEX

Resting CSI significantly positively correlated with outward deformation of the brainstem, right amygdala, right nucleus accumbens and bilateral pallidum nuclei (i.e. outward shape change) (Figure 3, Figure 4, Movie 2) (thresholded TFCE p<0.05).

[INSERT FIGURE 3 HERE]

[INSERT FIGURE 4 HERE]

[INSERT MOVIE 2 HERE FOR ONLINE VERSION]

PARASYMPATHTIC: CARDIAC VAGAL TONE

No significant positive correlations (i.e. outward deformation) between resting CVT and nuclei shape survived correction for multiple comparisons. Contrasting to sympathetic analyses however, resting CVT negatively correlated with inward deformation of the right amygdala and right pallidum (i.e. inward shape change of these two nuclei) (Figure 3, Figure 5, Movie 2) (thresholded TFCE p<0.05).

[INSERT FIGURE 5 HERE]

SUBCORTICAL VOLUMETRIC ANALYSIS

Firstly, to test the null hypothesis that volumes would not significantly differ between left or right sided subcortical nuclei, paired student's two-tailed *t* tests were performed to test for side differences. No significant differences were found between left and right sided nuclei volumes (all *p* values greater than 0.73). Furthermore, there was no association of CVT/CSI on total brain or total gray matter volumes (data not shown). Resting CVT was significantly positively correlated with the volume of the left and right putamen (r = 0.62, p=0.0047 and r =0.59, p=0.008, respectively). In addition, total brainstem volume positively correlated with resting CVT, albeit loosely so (r = 0.46, p=0.049) (Figure 6). In contrast, no significant correlation was observed between resting CSI and subcortical nuclei volume.

[INSERT FIGURE 6 HERE]

DISCUSSION

ASSOCIATION OF SUBCORTICAL NUCLEI SHAPE AND RESTING AUTONOMIC ACTIVITY

We have identified multiple subcortical nuclei whose shape deformation is significantly associated with differences in baseline autonomic indices. We have for the first time demonstrated that resting CSI positively correlates with outward deformation of the brainstem, right amygdala, right nucleus accumbens and bilateral pallidum, whilst resting CVT negatively correlates with inward deformation to the shape of the right pallidum and amygdala.

Several previous studies have documented the role of subcortical brain regions in autonomic function, and the modulation and maintenance of SNS tone has previously been associated with the brainstem, amygdala, nucleus accumbens and pallidum. An interesting study using a double-virus transneuronal labelling technique in Sprague Dawley rats, demonstrated that sympathetic neurons are localized to brainstem regions (Jansen, et al., 1995). Studies in rabbits and rats using regional cutaneous vascular flow, as a surrogate for sympathetic activity, demonstrated that neuronal blockade of the amygdala attenuated cutaneous vasoconstriction, thereby highlighting the importance of the amygdala in the sympathetic pathway (Blessing, 2003). Nalivaiko *et al.* have shown in animal models that the sympathetic-specific vasomotor response to electrical stimulation transverses through the amygdala and brainstem (raphe/parapyramidal neurons) to the peripheral target, as muscimol blockage at the raphe level abolished the cutaneous vascular response otherwise observed from amygdala stimulation (Nalivaiko and Blessing, 2001). Furthermore, the function of dopamine *efferent* neurons of the nucleus accumbens includes the modulation of sympathetic innervation in peripheral tissues (Saurer, et al., 2008), and a role for the pallidum in modulating sympathetic-induced salivary secretion has been demonstrated (Pazo, et al., 1981). In summary, previous studies support the notion that subcortical brain regions are implicated in SNS function, and our novel morphological data herein adds weight to this.

Previous studies investigating both structural and functional brain differences associated with parasympathetic activity have largely implicated cortical regions, such as the anterior cingulate cortex (ACC) (Kano, et al., 2014; Winkelmann, et al., 2016). However, the ACC has been associated with many processes (see http://neurosynth.org/analyses/terms/acc/) and therefore its role in modulating PNS function is unlikely to be specific (Yarkoni, et al., 2011).

Subcortical brain regions are also implicated in modulating PNS function, and the amygdala and pallidum have both previously been associated with core parasympathetic tone, albeit for disparate autonomic functions including metabolism, reward, emotion and motor response (Allen, et al., 2015; Critchley, 2005; Critchley and Harrison, 2013; Hawksley, et al., 2015; Macefield, 2009; McDougall, et al., 2014; Novac and Bota, 2014; Park and Thayer, 2014; Su, et al., 2015; Tanaka, et al., 2016). We have demonstrated that the amygdala and pallidum differ in shape depending on an individual's resting CVT. However, it remains uncertain whether subcortical morphology influences baseline autonomic tone, or whether the converse is true. It would therefore be premature to infer a direction of causality based upon our current findings.

In the context of disease, this study provides interesting insight. It has for some time been known that autonomic tone is perturbed in various neurological disorders. A key example includes that of ischaemic stroke, whereby numerous studies have shown a consequential disturbance in autonomic tone (Dutsch, et al., 2007; Mäkikallio, 2005; Palamarchuk, et al., 2013). Importantly, lacunar infarct strokes of subcortical regions such as the basal ganglia are associated with alteration to autonomic function (Dutsch, et al., 2007). These observations therefore support our data that these specific brain regions have an important role in autonomic regulation.

An additional aspect that makes our study unique is that most previous studies investigating brain structure and resting PNS tone solely investigated the total volume of specific regions. Whilst this method has been utilized in structural neuroimaging for some time and has indeed produced many interesting results, including those reported by (Winkelmann, et al., 2016),

the concept that regional structures are reducible to a single volume to correlate with a dynamic variable such as PNS or SNS tone is likely to represent an oversimplification. We suggest that one step to overcome this limitation is the advent of shape or vertex-wise analysis, which may offer greater insights into how specific structural disparities may link with physiological function. For instance, while volumetric brain differences may not be apparent when investigating a link with a given physiological variable, this may be due to combinations of inward and outward deformation changes that, when combined, nullify the result to a non-significant volume difference. This may thus limit our understanding of human physiology and brain structure and function.

PUTMAMEN VOLUME POSITIVELTY CORRELATES WITH RESTING VAGAL TONE

In our study, bilateral putamen volume was positively correlated with resting CVT, a region of the basal ganglia previously implicated in autonomic dysfunction such as that observed in Parkinson's disease (DeLong and Wichmann, 2007). For example, common 'non-motor' symptoms of Parkinson's disease include: i) autonomic disturbances including perturbed gastrointestinal motility, abnormalities in cardiac, urogenital, sudomotor, thermoregulatory, sleep and respiratory regulation; and ii) visceral pain, for which the vagal nerve holds a critical role (Mulak and Bonaz, 2015). Furthermore, a recent study in patients with obstructive sleep apnoea (OSA) provides an interesting example of autonomic function being associated with putamen volume (Kumar, et al., 2014). Specifically, global putamen volumes were reported to be higher in OSA patients compared to controls, but local volume analysis revealed additional areas of lower volume, hypothesised by the authors to in-part contribute to the apparent perturbation in autonomic function in OSA patients. This methodology is comparable to the vertex analyses we report, in that whilst a nucleus may have an overall

positive correlation with a given variable, there may in fact be small areas of this structure that negatively correlates with it. This highlights the importance of specific regional neuroimaging analyses, since additional important findings may otherwise be missed (such as the low volume areas in OSA patients reported by (Kumar, et al., 2014)). Furthermore, previous studies have described projections of the vagus nerve to the basal ganglia, using both functional MRI (Frangos, et al., 2015) and dopaminergic chromatography (Ziomber, et al., 2012). Nevertheless, our study is the first to illustrate an association between putamen volume and resting vagal tone in healthy controls. Coalescence of our shape and volume analysis findings with data from previous studies supports the proposition that basal ganglia nuclei, in particular the putamen and pallidum, are associated with PNS function (Pazo and Belforte, 2002).

LIMITATIONS

This study is not without limitations. Firstly, our sample size is relatively small, thereby reducing statistical power for complex analysis. However, a vast number of confounds of brain structure and resting autonomic tone have been either excluded (including anxiety, depression, hormonal factors, alcohol, caffeine and time of day) or have been included as covariates (gender and age) in the analysis. Therefore, even with this sample size, statistically robust results have been obtained illustrating the effect of resting CSI and CVT on subcortical nuclei shape. Secondly, it is possible that additional confounds of resting autonomic tone have not been screened or co-varied for. However, a large number of exclusion criteria and demographic covariates were added, all of which were chosen *a priori* from our previous autonomic research (Farmer, et al., 2014a; Farmer, et al., 2013a; Farmer, et al., 2014b), such that it is anticipated that the majority of basic individual demographical and

psychophysiological parameters are accounted for. Thirdly, the Bayesian Appearance Model analytical package used in its current form does not permit evaluation of the insula cortex for deformation changes contingent on a given variable (Patenaude, et al., 2011). Future studies should interrogate the insula cortex for structural changes correlative to resting autonomics. Lastly, this study was not designed to provide definitive evidence regarding causality of the observed association. Whilst we have observed a clear association between autonomic tone and brain structure, what remains unclear is as to whether subcortical shape 'shapes' autonomic tone, or rather the converse. This limitation warrants further study.

IMPLICATIONS FOR FUTURE STUDIES AND CONCLUSIONS

Arguably, one of the most inherent limitations of neuroimaging techniques are the effects of inter-individual variability and therefore it is not surprising that there exists a considerable research effort aiming to delineate these factors (Coen, et al., 2011; Farmer, et al., 2013a; Omran and Aziz, 2014; Ruffle, et al., 2015b). The putative factors proposed to account for this variability include, but are not limited to, demographic aspects and psychophysiological factors including not only personality traits (Coen, et al., 2011; Ruffle, et al., 2015b), but also more complex multifactorial endophenotypes for stress-events such as visceral pain (Farmer, et al., 2013a; Tracey, 2011). The identification of brain regions whose shape or volume is influenced by resting autonomic function supports the identification of resting autonomic activity as a further factor that, where available, should be controlled for. Importantly, it is also possible that autonomic differences have indeed contributed to, or even confounded, many previous findings. For example, a large proportion of neuroimaging studies that investigate either brain structure or function compare disease states characterised by chronic pain, such as IBS and fibromyalgia, and duly compare findings to those in healthy controls.

Notably, IBS and fibromyalgia have both been associated with perturbations in autonomic function (Mazurak, et al., 2012; Ruffle, et al., 2015a; Spaziani, et al., 2008). Furthermore, Farmer *et al*., have previously demonstrated that differences in both baseline and post-pain autonomic function influence brain activation to visceral pain (Farmer, et al., 2014a; Farmer, et al., 2013a). However, very few (if any) neuroimaging studies to date that have investigated or controlled for differences in baseline autonomic activity between groups.

In conclusion, our study provides novel evidence that resting autonomic state, by means of CSI and CVT measurement, is associated with differences in the shape or volume of subcortical nuclei. Given that perturbations in autonomic function occur in many disorders in which brain morphology is studied and abnormalities identified, it is therefore arguable that some of these morphological changes may be consequential to the disturbance in autonomic function associated with these disorders, or may at least be confounded by it. Resting autonomic tone should be controlled for as a covariate in future studies. Our data warrants further exploration in clinical cohorts and may provide further insights into the pathophysiology of disorders characterised by autonomic dysfunction.

ACKNOWLEDGEMENTS

This research/ADF was funded by a Medical Research Council project grant - Medical Research Council Grant Number - MGAB1A1R which was awarded to QA as principal investigator.

SW wishes to thank the UK Medical Research Council (MRC Grant Code: MR/N026969/1) and National Institute for Health Research (NIHR) Biomedical Research Centre for Mental Health at South London and Maudsley NHS Foundation Trust, King's College London for their continued support of our neuroimaging and pain projects

REFERENCES

Allen, B., Jennings, J.R., Gianaros, P.J., Thayer, J.F., Manuck, S.B. (2015) Resting high-frequency heart rate variability is related to resting brain perfusion. Psychophysiology, 52:277-87.

Benarroch, E.E., Opfer-Gehrking, T.L., Low, P.A. (1991) Use of the photoplethysmographic technique to analyze the Valsalva maneuver in normal man. Muscle & nerve, 14:1165-72.

Blessing, W.W. (2003) Lower brainstem pathways regulating sympathetically mediated changes in cutaneous blood flow. Cell Mol Neurobiol, 23:527-38.

Bonaz, B., Picq, C., Sinniger, V., Mayol, J.F., Clarencon, D. (2013) Vagus nerve stimulation: from epilepsy to the cholinergic anti-inflammatory pathway. Neurogastroenterol Motil, 25:208-21.

Bonaz, B., Sinniger, V., Pellissier, S. (2016) Anti-inflammatory properties of the vagus nerve: potential therapeutic implications of vagus nerve stimulation. The Journal of physiology, 594:5781-5790.

Botha, C., Farmer, A.D., Nilsson, M., Brock, C., Gavrila, A.D., Drewes, A.M., Knowles, C.H., Aziz, Q. (2015) Preliminary report: modulation of parasympathetic nervous system tone influences oesophageal pain hypersensitivity. Gut, 64:611-7.

Brar, T.K., Singh, K.D., Kumar, A. (2015) Effect of Different Phases of Menstrual Cycle on Heart Rate Variability (HRV). J Clin Diagn Res, 9:CC01-4.

Brock, C., Jessen, N., Brock, B., Jakobsen, P.E., Hansen, T.K., Rantanen, J.M., Riahi, S., Dimitrova, Y.K., Dons-Jensen, A., Aziz, Q., Drewes, A.M., Farmer, A.D. (2017) Cardiac vagal tone, a non-invasive measure of parasympathetic tone, is a clinically relevant tool in Type 1 diabetes mellitus. Diabet Med.

Chen, H.C., Yang, C.C., Kuo, T.B., Su, T.P., Chou, P. (2012) Cardiac vagal control and theoretical models of co-occurring depression and anxiety: a cross-sectional psychophysiological study of community elderly. BMC Psychiatry, 12:93.

Coen, S.J., Kano, M., Farmer, A.D., Kumari, V., Giampietro, V., Brammer, M., Williams, S.C., Aziz, Q. (2011) Neuroticism influences brain activity during the experience of visceral pain. Gastroenterology, 141:909-917 e1.

Critchley, H.D. (2005) Neural mechanisms of autonomic, affective, and cognitive integration. J Comp Neurol, 493:154-66.

Critchley, H.D., Harrison, N.A. (2013) Visceral influences on brain and behavior. Neuron, 77:624-38.

D'Agostino, R.B., Stephens, M.A. (1986) Goodness-of-fit techniques. New York. M. Dekker.

De Wandele, I., Rombaut, L., Leybaert, L., Van de Borne, P., De Backer, T., Malfait, F., De Paepe, A., Calders, P. (2014) Dysautonomia and its underlying mechanisms in the hypermobility type of Ehlers-Danlos syndrome. Semin Arthritis Rheum, 44:93-100.

Dean, D.J., Orr, J.M., Bernard, J.A., Gupta, T., Pelletier-Baldelli, A., Carol, E.E., Mittal, V.A. (2016) Hippocampal Shape Abnormalities Predict Symptom Progression in Neuroleptic-Free Youth at Ultrahigh Risk for Psychosis. Schizophr Bull, 42:161-9.

DeLong, M.R., Wichmann, T. (2007) Circuits and circuit disorders of the basal ganglia. Arch Neurol, 64:20-4.

Denver, J.W., Reed, S.F., Porges, S.W. (2007) Methodological issues in the quantification of respiratory sinus arrhythmia. Biol Psychol, 74:286-94.

Dutsch, M., Burger, M., Dorfler, C., Schwab, S., Hilz, M.J. (2007) Cardiovascular autonomic function in poststroke patients. Neurology, 69:2249-55.

Eckert, S., Horstkotte, D. (2002) Comparison of Portapres non-invasive blood pressure measurement in the finger with intra-aortic pressure measurement during incremental bicycle exercise. Blood pressure monitoring, 7:179-83.

European, Society, of, Cardiology. (1996) Heart rate variability: standards of measurement, physiological interpretation and clinical use. Task Force of the European Society of Cardiology and the North American Society of Pacing and Electrophysiology. Circulation, 93:1043-65.

Farmer, A.D., Coen, S.J., Kano, M., Naqvi, H., Paine, P.A., Scott, S.M., Furlong, P.L., Lightman, S.L., Knowles, C.H., Aziz, Q. (2014a) Psychophysiological responses to visceral and somatic pain in functional chest pain identify clinically relevant pain clusters. Neurogastroenterol Motil, 26:139-48.

Farmer, A.D., Coen, S.J., Kano, M., Paine, P.A., Shwahdi, M., Jafari, J., Kishor, J., Worthen, S.F., Rossiter, H.E., Kumari, V., Williams, S.C., Brammer, M., Giampietro, V.P., Droney, J., Riley, J., Furlong, P.L., Knowles, C.H., Lightman, S.L., Aziz, Q. (2013a) Psychophysiological responses to pain identify reproducible human clusters. Pain, 154:2266-76.

Farmer, A.D., Coen, S.J., Kano, M., Weltens, N., Ly, H.G., Botha, C., Paine, P.A., Oudenhove, L.V., Aziz, Q. (2014b) Normal values and reproducibility of the real-time index of vagal tone in healthy humans: a multi-center study. Annals of gastroenterology : quarterly publication of the Hellenic Society of Gastroenterology, 27:362-368.

Farmer, A.D., Coen, S.J., Kano, M., Worthen, S.F., Rossiter, H.E., Navqi, H., Scott, S.M., Furlong, P.L., Aziz, Q. (2013b) Psychological traits influence autonomic nervous system recovery following esophageal intubation in health and functional chest pain. Neurogastroenterol Motil, 25:950-e772.

Frangos, E., Ellrich, J., Komisaruk, B.R. (2015) Non-invasive Access to the Vagus Nerve Central Projections via Electrical Stimulation of the External Ear: fMRI Evidence in Humans. Brain stimulation, 8:624-36.

Frokjaer, J.B., Bergmann, S., Brock, C., Madzak, A., Farmer, A.D., Ellrich, J., Drewes, A.M. (2016) Modulation of vagal tone enhances gastroduodenal motility and reduces somatic pain sensitivity. Neurogastroenterol Motil.

Hawksley, J., Cavanna, A.E., Nagai, Y. (2015) The role of the autonomic nervous system in Tourette Syndrome. Front Neurosci, 9:117.

Hibino, G., Moritani, T., Kawada, T., Fushiki, T. (1997) Caffeine enhances modulation of parasympathetic nerve activity in humans: quantification using power spectral analysis. J Nutr, 127:1422-7.

Hoff, D.A., Brock, C., Farmer, A.D., Dickman, R., Ruffle, J.K., Shaker, A., Drewes, A.M. (2016) Pharmacological and other treatment modalities for esophageal pain. Annals of the New York Academy of Sciences.

Jansen, A.S., Nguyen, X.V., Karpitskiy, V., Mettenleiter, T.C., Loewy, A.D. (1995) Central command neurons of the sympathetic nervous system: basis of the fight-or-flight response. Science, 270:644-6.

Julu, P.O. (1992) A linear scale for measuring vagal tone in man. Journal of autonomic pharmacology, 12:109-15.

Julu, P.O., Hondo, R.G. (1992) Effects of atropine on autonomic indices based on electrocardiographic R-R intervals in healthy volunteers. Journal of neurology, neurosurgery, and psychiatry, 55:31-5.

Kano, M., Coen, S.J., Farmer, A.D., Aziz, Q., Williams, S.C., Alsop, D.C., Fukudo, S., O'Gorman, R.L. (2014) Physiological and psychological individual differences influence resting brain function measured by ASL perfusion. Brain structure & function, 219:1673-84.

Kollai, M., Kollai, B. (1992) Cardiac vagal tone in generalised anxiety disorder. Br J Psychiatry, 161:831-5.

Kumar, R., Farahvar, S., Ogren, J.A., Macey, P.M., Thompson, P.M., Woo, M.A., Yan-Go, F.L., Harper, R.M. (2014) Brain putamen volume changes in newly-diagnosed patients with obstructive sleep apnea. Neuroimage Clin, 4:383-91.

Little, C.J., Julu, P.O., Hansen, S., Reid, S.W. (1999) Real-time measurement of cardiac vagal tone in conscious dogs. The American journal of physiology, 276:H758-65.

Macefield, V.G. (2009) Developments in autonomic research: a review of the latest literature. Clin Auton Res, 19:193-6.

Mäkikallio, A. (2005) Cardiovascular autonomic and hormonal dysregulation in ischemic stroke with an emphasis on survival. International Journal of Circumpolar Health, 64:534-535.

Martinez-Martinez, L.A., Mora, T., Vargas, A., Fuentes-Iniestra, M., Martinez-Lavin, M. (2014) Sympathetic nervous system dysfunction in fibromyalgia, chronic fatigue syndrome, irritable bowel syndrome, and interstitial cystitis: a review of case-control studies. J Clin Rheumatol, 20:146-50.

Matteoli, G., Gomez-Pinilla, P.J., Nemethova, A., Di Giovangiulio, M., Cailotto, C., van Bree, S.H., Michel, K., Tracey, K.J., Schemann, M., Boesmans, W., Vanden Berghe, P., Boeckxstaens, G.E. (2014) A distinct vagal anti-inflammatory pathway modulates intestinal muscularis resident macrophages independent of the spleen. Gut, 63:938-48.

Mazurak, N., Seredyuk, N., Sauer, H., Teufel, M., Enck, P. (2012) Heart rate variability in the irritable bowel syndrome: a review of the literature. Neurogastroenterol Motil, 24:206-16.

McDougall, S.J., Munzberg, H., Derbenev, A.V., Zsombok, A. (2014) Central control of autonomic functions in health and disease. Front Neurosci, 8:440.

Mulak, A., Bonaz, B. (2015) Brain-gut-microbiota axis in Parkinson's disease. World J Gastroenterol, 21:10609-20.

Mumford, J.A., Poline, J.B., Poldrack, R.A. (2015) Orthogonalization of regressors in FMRI models. PLoS One, 10:e0126255.

Nalivaiko, E., Blessing, W.W. (2001) Raphe region mediates changes in cutaneous vascular tone elicited by stimulation of amygdala and hypothalamus in rabbits. Brain Res, 891:130-7.

Novac, A., Bota, R.G. (2014) Transprocessing: a proposed neurobiological mechanism of psychotherapeutic processing. Ment Illn, 6:5077.

Omran, Y.A., Aziz, Q. (2014) Functional brain imaging in gastroenterology: to new beginnings. Nat Rev Gastroenterol Hepatol, 11:565-576.

Palamarchuk, I., Kimpinski, K., Lippert, C., Hachinski, V. (2013) Nocturnal deterioration after ischemic stroke and autonomic dysfunction: hypothesis and implications. Cerebrovasc Dis, 36:454-61.

Park, G., Thayer, J.F. (2014) From the heart to the mind: cardiac vagal tone modulates top-down and bottom-up visual perception and attention to emotional stimuli. Frontiers in psychology, 5:278.

Patenaude, B., Smith, S.M., Kennedy, D.N., Jenkinson, M. (2011) A Bayesian model of shape and appearance for subcortical brain segmentation. Neuroimage, 56:907-22.

Pazo, J.H., Belforte, J.E. (2002) Basal Ganglia and Functions of the Autonomic Nervous System. Cellular and Molecular Neurobiology, 22:645-654.

Pazo, J.H., Tumilasci, O.R., Medina, J.H. (1981) Studies on the mechanisms of L-dopa-induced salivary secretion. European journal of pharmacology, 69:255-61.

Ruffle, J., Shah, M., Monro, J., Julu, P. (2015a) Pattern Of Dysautonomia In Patients With Functional Gastrointestinal Disorders. Autonomic Neuroscience: Basic and Clinical, 192:119.

Ruffle, J.K., Aziz, Q., Farmer, A.D. (2017) Neuroimaging of vagal nerve stimulation; are we missing a trick? Pain, In Press.

Ruffle, J.K., Farmer, A.D., Kano, M., Giampietro, V., Aziz, Q., Coen, S.J. (2015b) The influence of extraversion on brain activity at baseline and during the experience and expectation of visceral pain. Personality and Individual Differences, 74:248-253.

Saurer, T.B., Ijames, S.G., Carrigan, K.A., Lysle, D.T. (2008) Neuroimmune mechanisms of opioid-mediated conditioned immunomodulation. Brain Behav Immun, 22:89-97.

Schlereth, T., Birklein, F. (2008) The sympathetic nervous system and pain. Neuromolecular Med, 10:141-7.

Smith, S.M., Jenkinson, M., Woolrich, M.W., Beckmann, C.F., Behrens, T.E., Johansen-Berg, H., Bannister, P.R., De Luca, M., Drobnjak, I., Flitney, D.E., Niazy, R.K., Saunders, J., Vickers, J., Zhang, Y., De Stefano, N., Brady, J.M., Matthews, P.M. (2004) Advances in functional and structural MR image analysis and implementation as FSL. Neuroimage, 23 Suppl 1:S208-19.

Spaziani, R., Bayati, A., Redmond, K., Bajaj, H., Mazzadi, S., Bienenstock, J., Collins, S.M., Kamath, M.V. (2008) Vagal dysfunction in irritable bowel syndrome assessed by rectal distension and baroreceptor sensitivity. Neurogastroenterol Motil, 20:336-42.

Su, J., Tanaka, Y., Muratsubaki, T., Kano, M., Kanazawa, M., Fukudo, S. (2015) Injection of corticotropin-releasing hormone into the amygdala aggravates visceral nociception and induces noradrenaline release in rats. Neurogastroenterology & Motility, 27:30-39.

Tanaka, Y., Kanazawa, M., Kano, M., Morishita, J., Hamaguchi, T., Van Oudenhove, L., Ly, H.G., Dupont, P., Tack, J., Yamaguchi, T., Yanai, K., Tashiro, M., Fukudo, S. (2016) Differential Activation in Amygdala and Plasma Noradrenaline during Colorectal Distention by Administration of Corticotropin-Releasing Hormone between Healthy Individuals and Patients with Irritable Bowel Syndrome. PLoS One, 11:e0157347.

Toichi, M., Sugiura, T., Murai, T., Sengoku, A. (1997) A new method of assessing cardiac autonomic function and its comparison with spectral analysis and coefficient of variation of R-R interval. Journal of the autonomic nervous system, 62:79-84.

Tracey, I. (2011) Can neuroimaging studies identify pain endophenotypes in humans? Nat Rev Neurol, 7:173-81.

Vinik, A.I., Maser, R.E., Mitchell, B.D., Freeman, R. (2003) Diabetic autonomic neuropathy. Diabetes Care, 26:1553-79.

Volkman, J.E., DeRycke, E.C., Driscoll, M.A., Becker, W.C., Brandt, C.A., Mattocks, K.M., Haskell, S.G., Bathulapalli, H., Goulet, J.L., Bastian, L.A. (2015) Smoking Status and Pain Intensity Among OEF/OIF/OND Veterans. Pain medicine (Malden, Mass.), 16:1690-6.

Winkelmann, T., Thayer, J.F., Pohlack, S., Nees, F., Grimm, O., Flor, H. (2016) Structural brain correlates of heart rate variability in a healthy young adult population. Brain structure & function.

Winkler, A.M., Ridgway, G.R., Webster, M.A., Smith, S.M., Nichols, T.E. (2014) Permutation inference for the general linear model. Neuroimage, 92:381-97.

Yarkoni, T., Poldrack, R.A., Nichols, T.E., Van Essen, D.C., Wager, T.D. (2011) NeuroSynth: a new platform for large-scale automated synthesis of human functional neuroimaging data. Frontiers in Neuroinformatics.

Zhang, T., Shaw, M., Humphries, J., Sachdev, P., Anstey, K.J., Cherbuin, N. (2016) Higher fasting plasma glucose is associated with striatal and hippocampal shape differences: the 2sweet project. BMJ Open Diabetes Res Care, 4:e000175.

Zigmond, A.S., Snaith, R.P. (1983) The hospital anxiety and depression scale. Acta psychiatrica Scandinavica, 67:361-70.

Ziomber, A., Thor, P., Krygowska-Wajs, A., Zalecki, T., Moskala, M., Romanska, I., Michaluk, J., Antkiewicz-Michaluk, L. (2012) Chronic impairment of the vagus nerve function leads to inhibition of dopamine but not serotonin neurons in rat brain structures. Pharmacol Rep, 64:1359-67.

TABLES & FIGURES

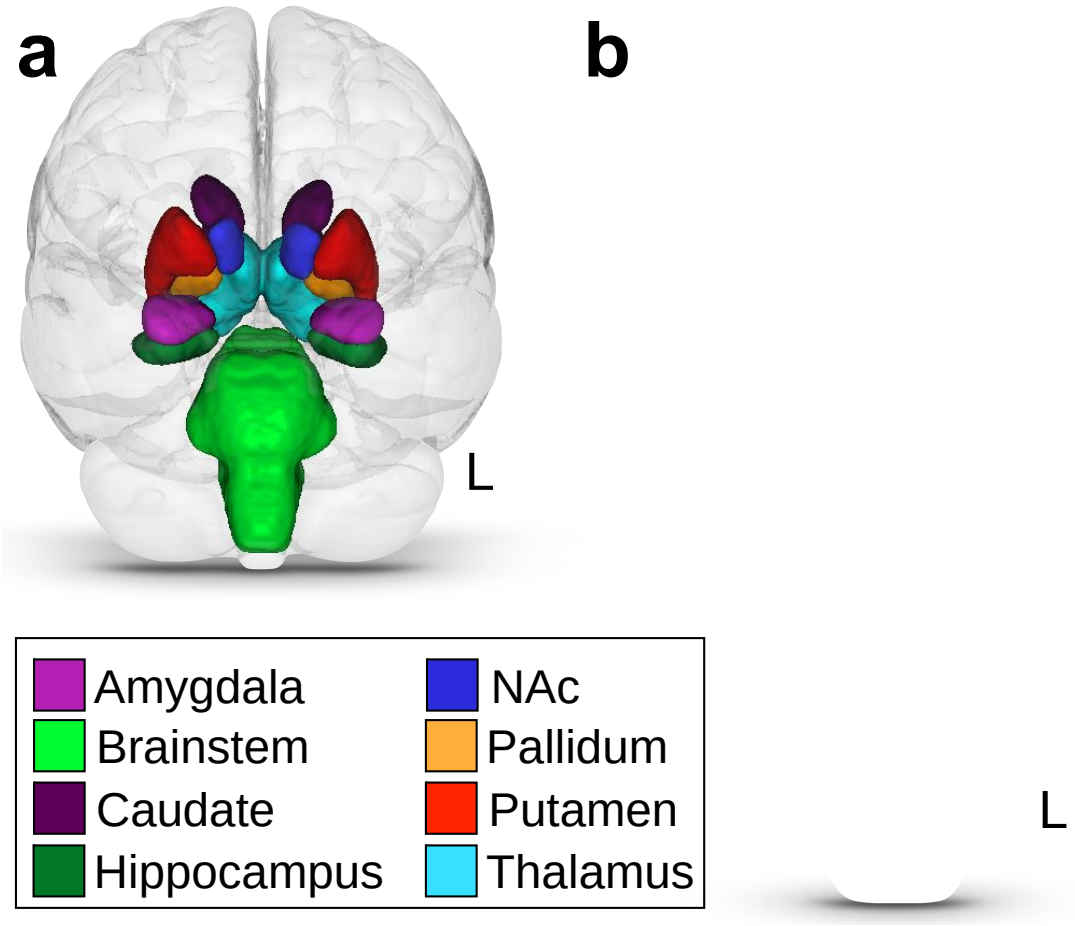

Figure 1: Subcortical segmentation for shape and volumetric analysis

Using FSL-FIRST, brain subcortical nuclei were segmented into 15 different regions. These were the bilateral amygdala, caudate, hippocampus, nucleus accumbens, pallidum, putamen, thalamus, and whole brainstem. a) Example of segmentation of the aforementioned nuclei of a single subject with structural brain scan superimposed, anterior view. b) Enlarged anterior view of nuclei segmentation, without superimposed brain so as to display all regions. Brain regions are similarly color coded for simplicity as in all other figures and supplementary videos. Abbreviations: L, left; NAc, nucleus accumbens.

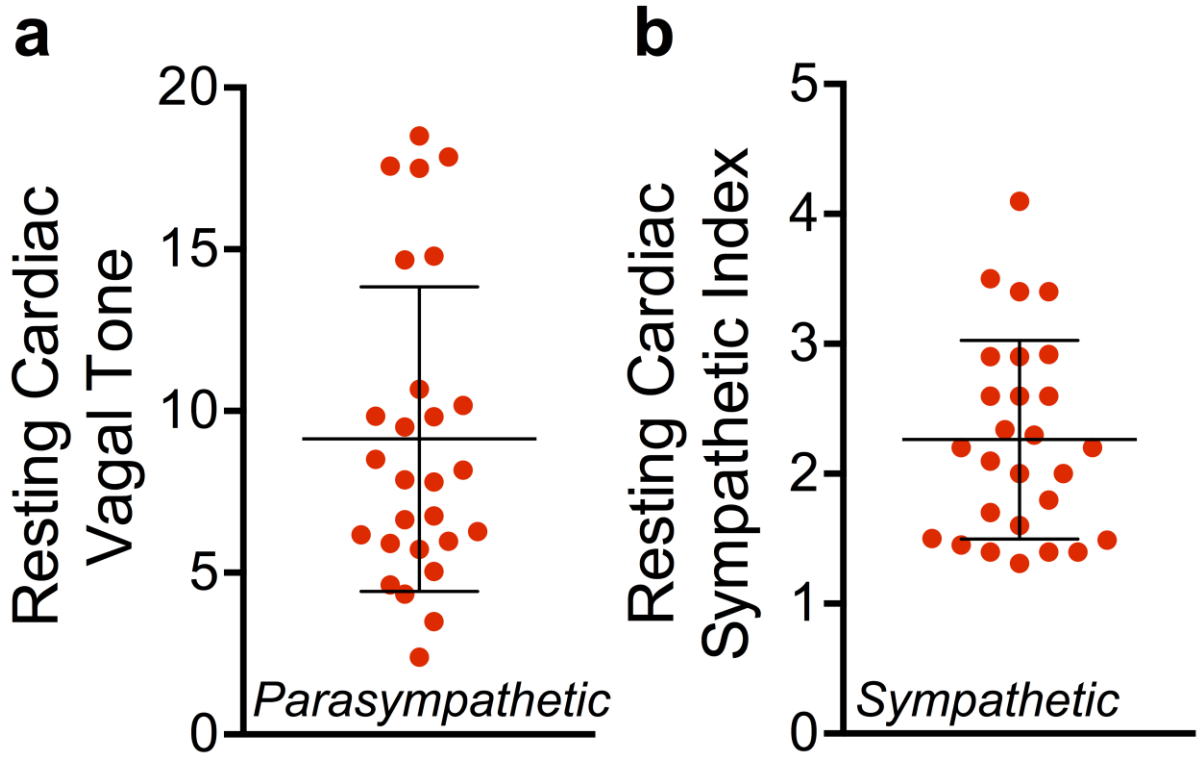

Figure 2: Cohort resting sympathetic and parasympathetic tone

Graph illustrating spread of resting CVT (a) and CSI (b) values (n=27). Red circles indicate individual resting CSI and CVT values, whilst bars display mean ± standard deviation. Abbreviations: CSI, cardiac sympathetic index; CVT, cardiac vagal tone.

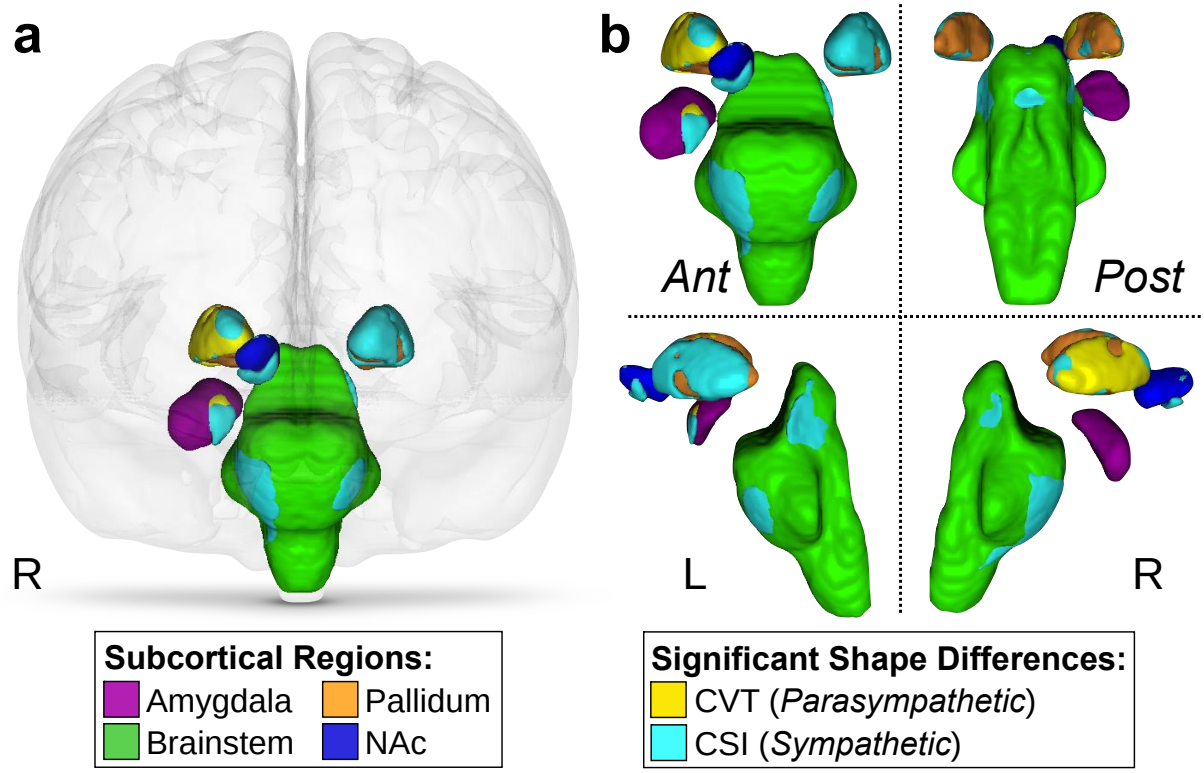

Figure 3: **Subcortical nuclei shape differs depending on resting sympathetic and parasympathetic tone**

Visualization of the subcortical brain regions which display a significant outward deformation (outward shape change) positively correlated to resting CSI, and significant inward deformation (inward shape change) negatively correlated to resting CVT. a) Anterior illustration with transparent brain superimposed. b) Anterior, posterior, left and right visualization of significant shape differences. Brain regions are similarly color coded for simplicity as in all other figures and supplementary videos. Turquoise components indicate the aspects whereby significant positive deformation (outward shape change) was associated with resting CSI, whilst yellow components of the nuclei indicate the aspects whereby significant negative deformation (inward shape change) negatively correlated to resting CVT. Abbreviations: CVT, cardiac vagal tone; L, left; NAc, nucleus accumbens; R, right.

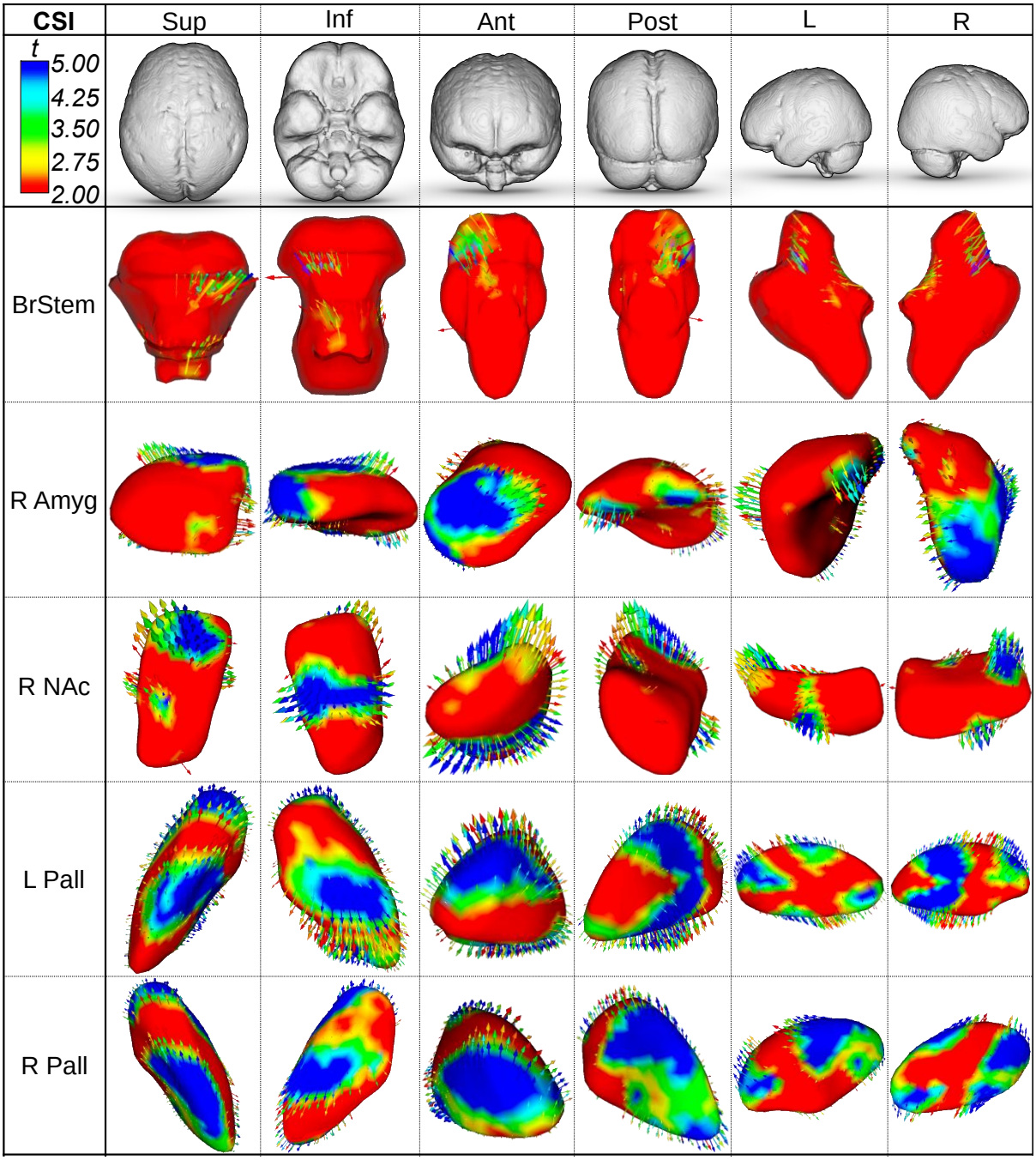

Figure 4: **Specific localization of significant deformation changes associated with resting cardiac sympathetic index**

Figure displaying specific areas of nuclei shape variation, depending on resting CSI. Only nuclei which survive statistical correction with multiple comparisons are displayed, and are that of the brainstem, right amygdala, right NAc and bilateral pallidum. Of note, all significant shape changes are that of outward deformation (outward shape change) with rising CSI. Multiple

views are displayed, and are signified across columns (superior, inferior, anterior, posterior, left, right). Three-dimensional brain template is provided for simplification of the given view. Subcortical nuclei are displayed with standard color scale. Color bar indicates *t* value from the given contrast, where blue indicates areas of higher significance and red areas of less significance. Arrows indicate the direction of shape deformation. Abbreviations: Ant, anterior; Amyg, amygdala; BrStem, brainstem; CSI, cardiac sympathetic index; Inf, inferior; L, left; NAc, nucleus accumbens; Pall, pallidum; Post, posterior; R, right; Sup, superior.

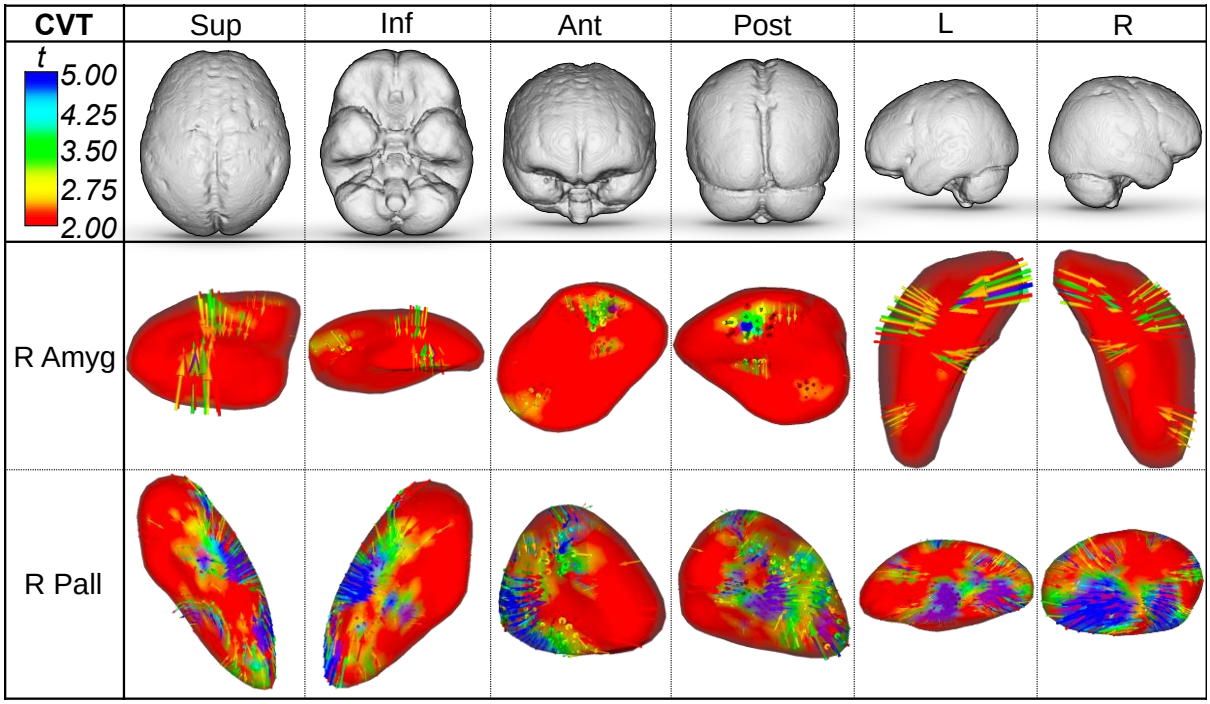

Figure 5: **Specific localization of significant deformation changes associated with resting cardiac vagal tone**

Figure displaying specific areas of nuclei shape variation, depending on resting CVT. Only nuclei which survive statistical correction with multiple comparisons are displayed, and are that of the right amygdala and right pallidum. Of note, all significant shape changes are that of inward deformation (inward shape change) with CVT. Therefore, for ease of illustration nuclei transparency is partially added. Multiple views are displayed, and are signified across columns (superior, inferior, anterior, posterior, left, right). Three-dimensional brain template is provided for simplification of the given view. Subcortical nuclei are displayed with standard color scale. Color bar indicates *t* value from the given contrast, where blue indicates areas of higher significance and red areas of less significance. Arrows indicate the direction of shape deformation. Abbreviations: Ant, anterior; Amyg, amygdala; CVT, cardiac vagal tone; Inf, inferior; L, left; Pall, pallidum; Post, posterior; R, right; Sup, superior.

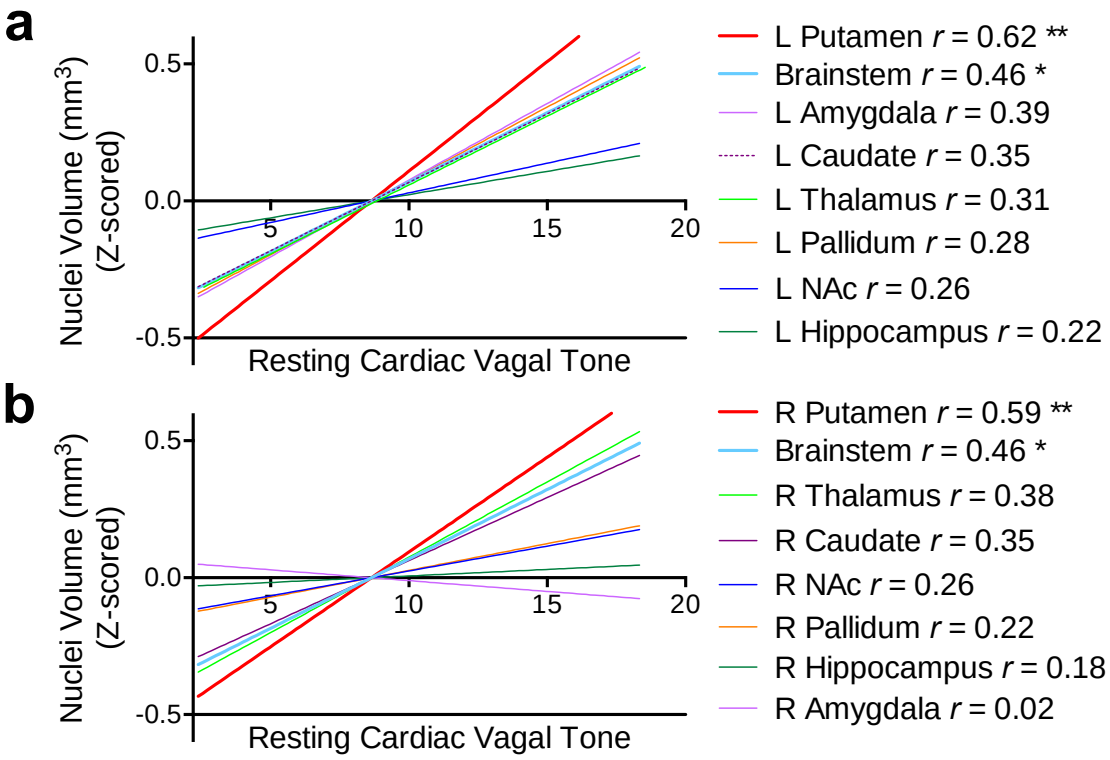

Figure 6: Putamen volume is highly correlated with resting cardiac vagal tone

Volumetric analyses were also performed of the segmented subcortical brain regions for all subjects. This outputs a single volumetric reading in mm^3. Figure displays nuclei volume for both a) left and b) right sided subcortical nuclei, and their correlation to resting CVT. Correlative *r* values are denoted at the right of the figure, in addition to their degree of significance as per conventional asterisks; * equates to $p < 0.05$; ** equates to $p < 0.01$. Volumes were z-scored so as to adjust for the disparity in size between the different nuclei for graph visualization purposes. Brain regions are similarly color coded for simplicity as in all other figures and supplementary videos. Of note, we report strong positive correlations between the volume of both the left and right putamen to resting vagal tone, but in addition a weak correlation with total brainstem volume. Left caudate and thalamic correlations were highly similar, thus a disparate line overlay has been used for ease of viewing. No brain regions display significant correlations of CSI to subcortical brain volumes. Abbreviations: L, left; NAc, nucleus accumbens; R, right.

TABLE 1

Cohort demographic & autonomic data

Variable	Mean ± SD
Demographical	
Age (years)	29.81 ± 8.35
Gender (M / F)	14 M, 13 F
Autonomic	
Resting HR (bpm)	68.12 ± 10.65
Resting CVT (LVS)	9.13 ± 4.70
Resting CSI (ratio)	2.26 ± 0.76
Systolic Blood	139 ± 34.70
Diastolic Blood	66 ± 15.66

Table 1: Cohort demographic & autonomic data

Cohort demographical and autonomic data for all subjects (n=27). Variables described as mean ± standard deviation. Of note, CVT lies on a linear vagal scale, whilst resting CSI is expressed as a ratio of R-R intervals. Abbreviations: BPM, beats per minute; CVT, cardiac vagal tone; CSI, cardiac sympathetic index; F, female; M, male; SD, standard deviation; LVS, linear vagal scale.

Suppl Movie 1: Three-dimensional video representation of subcortical segmentation for shape and volumetric analysis

Using FSL-FIRST, brain subcortical nuclei were segmented into 15 different regions. Of note, these were the bilateral amygdala, caudate, hippocampus, nucleus accumbens, pallidum, putamen, thalamus, and whole brainstem. Initial video illustrates orientation markers for simplicity. Brain regions are similarly color coded for simplicity as in all other figures and supplementary videos. Abbreviations: A, anterior; I, inferior; L, left; NAc, nucleus accumbens; P, posterior; R, right.

Suppl Movie 2: Three-dimensional video representation of results: subcortical nuclei shape is significantly different depending on resting sympathetic and parasympathetic tone

Visualization of the subcortical brain regions which display a significant outward deformation (outward shape change) positively correlated to resting CSI, and significant inward deformation (inward shape change) negatively correlated to resting CVT. Brain regions are similarly color coded for simplicity as in all other figures and supplementary videos. Turquoise components indicate the aspects whereby significant positive deformation (outward shape change) was associated with resting CSI, whilst yellow components of the nuclei indicate the aspects whereby significant negative deformation (inward shape change) negatively correlated to resting CVT. Abbreviations: CSI, cardiac sympathetic index; CVT, cardiac vagal tone; NAc, nucleus accumbens.